Robotic Tactile Recognition of Pseudorandom Encoded Objects

Emil M. Petriu, *Fellow, IEEE*, Stephen K. S. Yeung, Sunil R. Das, *Life Fellow, IEEE*, Ana-Maria Cretu, *Student Member, IEEE*, and Hans J. W. Spoelder

***Abstract*—This paper discusses an original model-based method for blind robotic tactile recognition of three-dimensional objects. Conveniently shaped geometric symbols representing terms of a *pseudorandom array* (PRA) are embossed on object surfaces. Symbols recovered by tactile probing are recognized using a neural network and then clustered in a PRA window that contains enough information to fully identify the absolute coordinates of the recovered window within the encoding PRA. By knowing how different object models were mapped to the PRA, it is possible to unambiguously identify the object face and the exact position of the recovered symbols on the face.**

***Index Terms*—Object recognition, pseudorandom arrays, tactile system, three-dimensional object model.**

I. Introduction

ROBOTIC tactile sensing systems for object recognition essentially emulate biological haptic perception mechanisms, [1], [2]. Pattern recognition is a more complicated task in the case of tactile perception than in visual perception, as there are a number of difficult-to-control factors affecting the quality of tactile images such as complex strain-stress relationship in the elastic overlay, amount of force, and contact angle during the tactile perception process. Due to these limitations, tactile sensing is mostly used as an aid to vision only in object recognition applications [3].

However, there are situations when visual information is not available, such as in the case of underwater robotics or manipulation of objects by blind persons [4], [5], where touch remains the only sensing modality available for the recognition of the objects encountered in the working environment.

Jurczyk and Loparo present in [6] a model-based tactile object recognition method where objects are recognized by correlating a set of measured tactile features with a series of typical tactile features from a library of object models.

Germagnoli and Magenes discuss in [7] a tactile object identification technique based on the neural network (NN) recognition of five tactile primitives similar to the human fingertip exploration of prism-shaped rigid objects. A robotic tactile probe tracks all the edges of the object, an NN is used to classify the polygonal shapes of each face of the object, and finally another NN recognizes the shape of the whole object.

This paper discusses an original model-based method for blind tactile recognition of three-dimensional (3-D) objects. Conveniently shaped geometric symbols representing terms of a *pseudorandom array* (PRA) are embossed on object surfaces. Symbols recovered by tactile probing are recognized using a neural network and then clustered in a PRA window that contains enough information to fully identify the absolute coordinates of the recovered window within the encoding PRA. By knowing how different object models were mapped to the PRA, it is possible to unambiguously identify the object face and the exact position of the recovered symbols on the face.

The encoded surfaces should either be flat or have a curvature radius large enough to be inspected by a planar tactile array probe.

II. Pseudorandom Array Encoding

The proposed tactile object recognition paradigm can be formally stated as follows: "Given a set of 3-D objects having their faces embossed with symbols that represent the terms of a PRA according to a preestablished mapping, find a tactile image processing and code recovery method for the unambiguous identification of the inspected object face and the exact position of the probed area on the face."

A. Pseudorandom Arrays

A generic *pseudorandom sequence* (PRS) has multivalued elements taken from an alphabet of q symbols, where q is a prime or a power of a prime. As a side note, *pseudorandom binary sequences* (PRBSs) are a particular case of PRSs when $q = 2$.

A $(q^n - 1)$-term PRS is generated by an n-position shift register with a feedback path specified by a primitive polynomial

$$h(x) = x^n + h_{n-1} \cdot x^{n-1} + \cdots + h_1 \cdot x + h_0 \quad (1)$$

of degree n with coefficients from the Galois field $\mathrm{GF}(q)$.

When q is a power of a prime, $q = p^m$, the Galois field elements are expressed as the first $q-1$ powers of some primitive element, labeled here by the letter "A"

$$\mathrm{GF}(q) = \{0, 1, A, A^2, \ldots, A^{q-2}\} \quad (2)$$

as illustrated in Table I [8].

Manuscript received June 15, 2003; revised May 8, 2004. This work was supported in part by the Natural Sciences and Engineering Research Council of Canada and the Canadian Space Agency.

E. M. Petriu, S. R. Das, and A.-M. Cretu are with the University of Ottawa, Ottawa, ON K1N 6N5, Canada.

S. K. S. Yeung is with The Chinese University of Hong Kong, Hong Kong.

H. J. W. Spoelder is with The Free University of Amsterdam, Amsterdam, The Netherlands.

Digital Object Identifier 10.1109/TIM.2004.834100

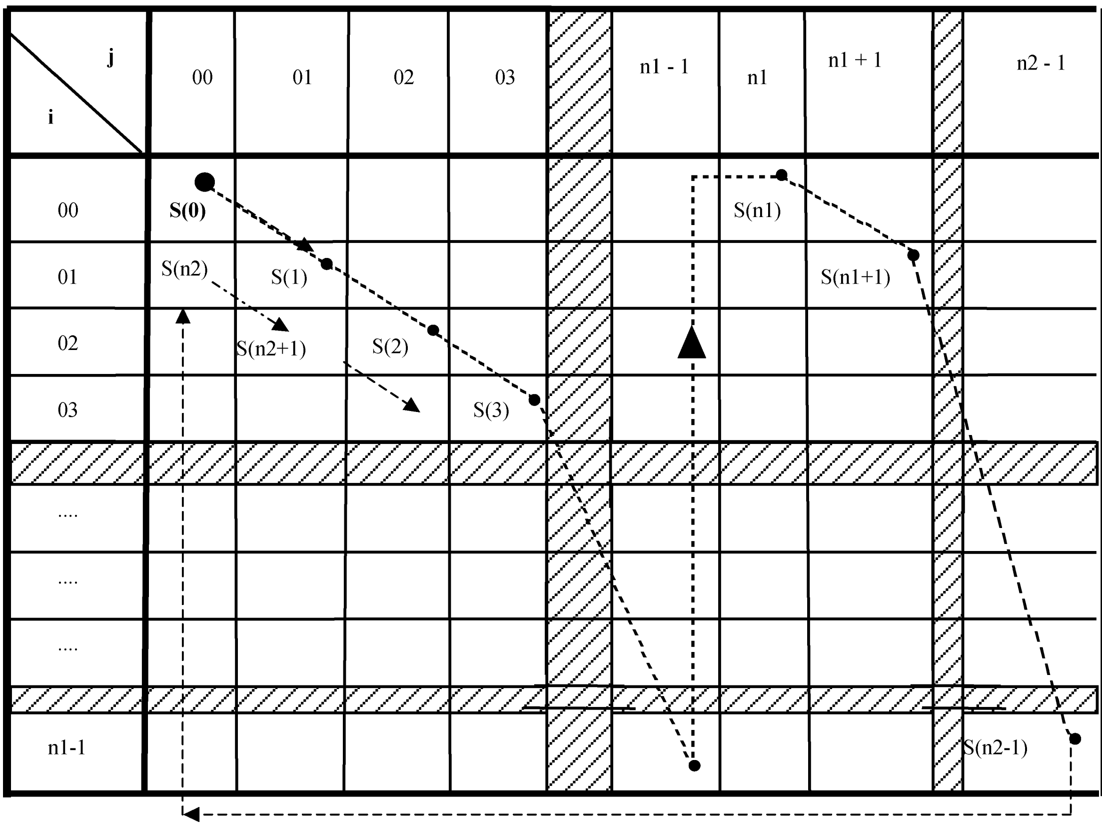

Fig. 1. PRA generation by diagonal folding of a PRS.

TABLE I
PRIMITIVE POLYNOMIALS OVER GF(q) $= \{0, 1, A, A^2, \ldots, A^{q-2}\}$

n	q=3	q=4	q=8
2	x^2+x+2	x^2+x+A	x^2+Ax+A
3	x^3+2x+1	x^3+x^2+x+A	x^3+x+A
4	x^4+x+2	$x^4+x^2+Ax+A^2$	x^4+x+A^3
5	x^5+2x+1	x^5+x+A	$x^5+x^2+x+A^3$
6	x^6+x+2	x^6+x^2+x+A	x^6+x+A

A PRA can be obtained by properly folding, as shown in Fig. 1, a PRS defined by the primitive polynomial $h(x)$ of degree n over GF(q), of length $q^n - 1$ [9]. The dimensions of the resulting PRA are

$$n1 = q^{k1} - 1 \tag{3}$$

$$n2 = \frac{(q^n - 1)}{n1} \tag{4}$$

where

$$k_1 k_2 = n. \tag{5}$$

According to the PRA "window property," any nonzero pattern seen through a $k1$-by-$k2$ window sliding over the array is unique and may fully identify the window's absolute coordinates (i, j) within the PRA [8].

The resulting "pseudorandom/natural" code conversion is implemented as a memory stored table.

Fig. 2 shows as an example a 15-by-17 PRA obtained by folding a 255-element PRS defined over GF(4), with $q = 4$, $n = 4$, $k1 = 2$, $k2 = 2$, $n1 = q^{k1} - 1 = 15$, and $n2 = (q^n - 1)/n1 = 17$ [10].

The contents of any 2-by-2 window are unique allowing for an unequivocally recovery of the absolute line and column coordinates of the window. For instance, the 2-by-2 window marked in bold in Fig. 2 (A^2, A in the first row, and A^2, 1 in the second row) is not repeated anywhere within the 15-by-17 PRA. These window contents are unequivocally associated to the row–column coordinates $(i = 6, j = 5)$ of the upper left corner of this window within PRA (having $i = 0$ for its top row, and $j = 0$ for its most left column, as defined in Fig. 1).

B. Encoding Object Faces

Specially designed symbols representing PRA code elements are embossed on the object's faces. For convenient recovery by tactile probing and pattern recognition, the shape of these symbols has been selected to meet the following conditions.

1) There is enough information at the symbol level to provide an immediate indication of the grid orientation.
2) The symbol recognition procedure is invariant to position and orientation.
3) The symbols have particular shapes so that the other objects in the scene will not be mistaken for encoding symbols.

0	A	1	A^2	A	A^2	A^2	A^2	1	1	A^2	A^2	A^2	A	A^2	1	A
0	0	1	A^2	A^2	A	1	0	A^2	A^2	0	1	A	A^2	A^2	1	0
0	A^2	0	0	A	A	A^2	1	A^2	A^2	1	A^2	A	A	0	0	A^2
0	1	A	1	A	0	A^2	A	0	0	A	A^2	0	A	1	A	1
0	A^2	A^2	A	0	A^2	0	1	1	1	1	0	A^2	0	A	A^2	A^2
0	A^2	A	1	A^2	1	1	1	A	A	1	1	1	A^2	1	A	A^2
0	0	A	1	1	**A^2**	**A**	0	1	1	0	A	A^2	1	1	A	0
0	1	0	0	A^2	**A^2**	**1**	A	1	1	A	1	A^2	A^2	0	0	1
0	A	A^2	A	A^2	0	1	A^2	0	0	A^2	1	0	A^2	A	A^2	A
0	1	1	A^2	0	1	0	A	A	A	A	0	1	0	A^2	1	1
0	1	A^2	A	1	A	A	A	A^2	A^2	A	A	A	1	A	A^2	1
0	0	A^2	A	A	1	A^2	0	A	A	0	A^2	1	A	A	A^2	0
0	A	0	0	1	1	A	A^2	A	A	A^2	A	1	1	0	0	A
0	A^2	1	A^2	1	0	A	1	0	0	1	A	0	1	A^2	1	A^2
0	A	A	1	0	A	0	A^2	A^2	A^2	A^2	0	A	0	1	A	A

Fig. 2. 15-by-17 PRA with entries from the Galois field GF$(4) = \{0, 1, A, A^2\}$.

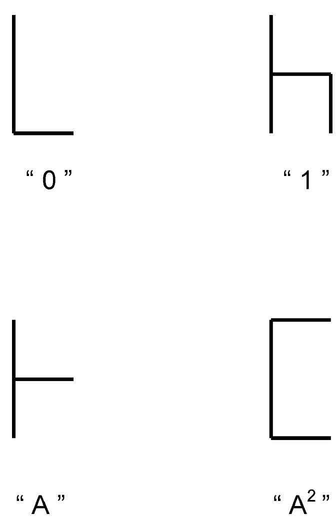

Fig. 3. The shape of the four code symbols used to emboss the elements of the PRA defined over GF(4) on object faces.

As an example, Fig. 3 shows the shape of the four symbols chosen in this paper to represent the elements of the PRA given in Fig. 2, defined over GF$(4) = \{0, 1, A, A^2\}$.

The features used to recover the position and orientation of the embossing symbols are [11]:

1) the x and y coordinates of the symbol position;
2) the directions of the symbol x and y axes;
3) the distances along the symbol axes to the neighboring symbols.

The unfolded faces of the objects are mapped on the physical layout of the encoding PRA as illustrated in Fig. 4. We are using “winged edge” geometric models [12] for the encoded objects. Each edge has four links associated specifying the two object faces separated by that edge and two vertices delimiting the edge. The mapping of the winged-edge object models to the encoding PRA is implemented as a relational database.

Usually, only part of the encoding symbols marked on the explored object surface is actually recognized. Based on the recognized symbols, a portion of the PRA can be reconstructed and then inspected to find a complete $k1$-by-$k2$ window.

The pseudorandom/natural code conversion of the recovered window contents yields the (i, j) coordinates of the origin of that window within the encoding PRA [10], [11]. Searching the relational database that stores the object geometry/PRA mapping for the location of the recovered PRA coordinates on the object surface, it becomes possible to identify both the object and the object face. This database search also gives the position of the recovered window on the identified object face.

III. Robotic Tactile Probing

The robotic tactile probing system, shown in Fig. 5, consists of a five-axis commercial robot arm, instrumented passive compliant wrist, and a tactile probe consisting of a tactile sensor with an elastic overlay [13], [14]. Under the action of the force exerted by the robot arm, the tactile probe is pressed onto the object surface in such a way that the 3-D geometric profile of this surface indents the overlay. The resulting stress profile produced in the elastic overlay is transmitted to the force-sensitive tactile sensor, producing a set of measurement data that represent an image of the geometric profile of the investigated object face.

The compliant wrist allows the tactile sensor to accommodate the constraints of the explored object face. Linear position sensors placed on all four sides of the instrumented passive-compliant wrist provide, along with the shaft encoders in the robot’s joints, the kinesthetic component of the haptic information.

The tactile sensor consists of a 16-by-16 matrix of force sensing resistor (FSR) elements spaced 1.5875 mm (1/16 in) apart on a 645.16 mm^2 (1 in^2) area. The elastic overlay consists of a relatively thin membrane with protruding round tabs sitting on top of each node of the FSR matrix providing a de facto

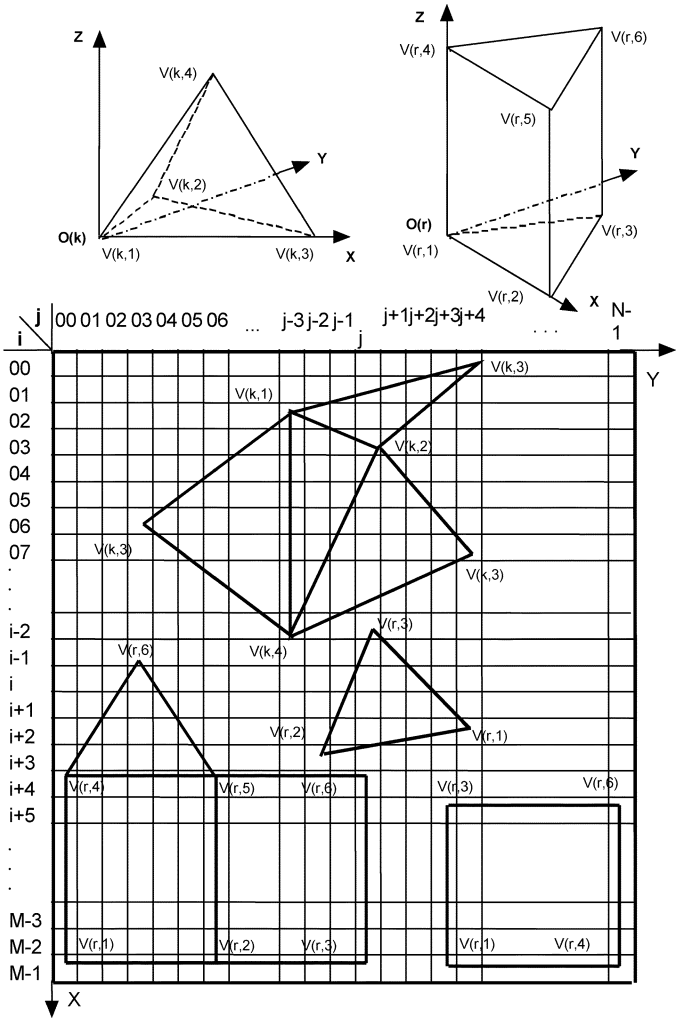

Fig. 4. 3-D object models are unfolded and mapped to the encoding PRA.

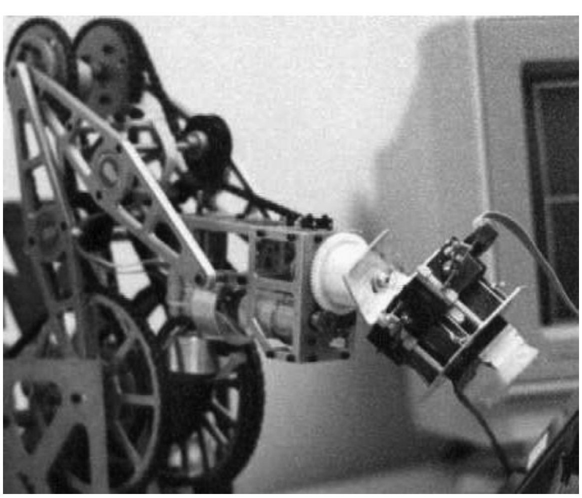

Fig. 5. The robotic tactile probing system.

spatial sampling. Each tab can expand laterally without any stress allowing for a proportional relationship between the displacement in the normal direction and the resulting stress component in each tab. As a result, the tactile probe output is a 16-by-16 array of data that represent normal components of the 3-D geometric profile of the investigated object surface $\{z(i\_ts, j\_ts) | i\_ts = 1, 2, \ldots, 16; j\_ts = 1, 2, \ldots, 16\}$, where i_ts and j_ts are the column and row coordinates of the tactile sensor matrix.

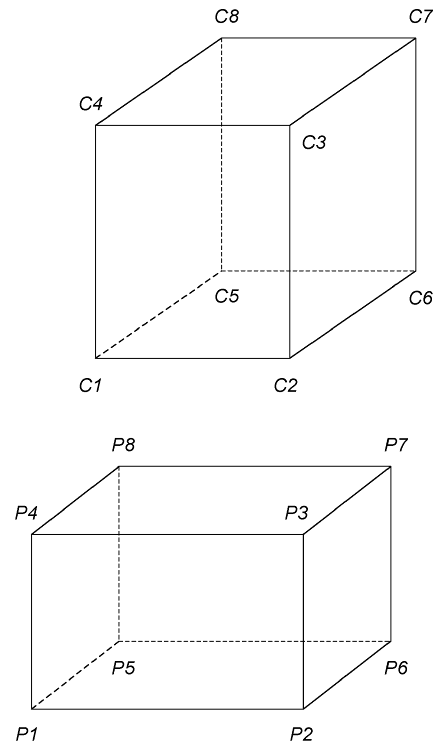

Fig. 6. The vertex definition of the 3-D objects, a cube and a parallelepiped, used in experiments.

IV. Experimental Results

We used in our experiments two 3-D polyhedral objects: a cube having 127 mm (5 in) long sides and a parallelepiped 177.8 mm (7 in) in length, 101.6 mm (4 in) in width, and 95.25 mm (3 3/4 in) in height. Fig. 6 shows the vertex defined geometric models of these two objects: {C1, C2, C3, C4, C5, C6, C7, C8} for the cube and {P1, P2, P3, P4, P5, P6, P7, P8} for the parallelepiped.

Fig. 7 shows the physical layout of the 15-by-17 PRA with the code elements represented by the four embossing symbols. The 19.05 mm (3/4 in) tall, 38.1 mm (1 1/2 in) wide, and 1.5875 mm (1/16 in) thick symbols are set 25.4 mm (1 in) apart in the horizontal direction and 31.75 mm (1 1/4 in) apart in the horizontal direction.

The unfolded faces of the two objects used in the experiments were mapped to the physical layout of the 15-by-17 PRA as illustrated in Fig. 8. As the PRA symbols embossed on the objects are 19.05 mm (3/4 in) tall and 38.1 mm (1 1/2 in) wide, any of them could be fully covered by the sensing area (1 in^2) of the tactile probe. As an example, Fig. 9 shows a view of the PRA encoded cube.

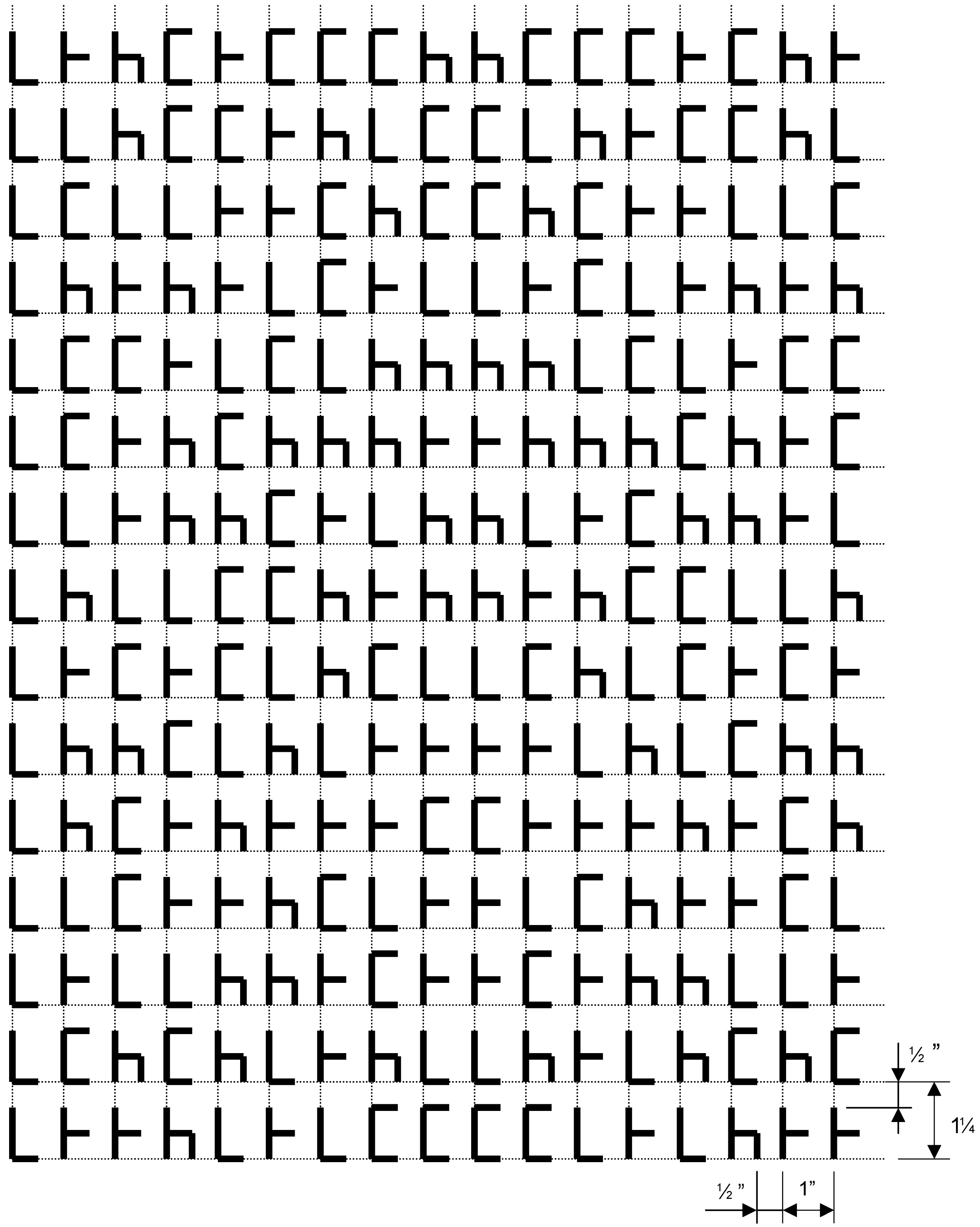

Fig. 7. The physical layout of the 15-by-17 PRA with the code elements represented by the four embossing symbols. The symbols are set 25.4 mm (1 in) apart in the horizontal direction and 31.75 mm (1 1/4 in) apart in the horizontal direction, providing a clear space of 12.7 mm (1/2 in) between symbols in both directions.

A composite tactile image is assembled incrementally from a sequence of overlapping tactile probe images. A 2-D cross-correlation algorithm is used to correct the misalignment errors of successive images that occur during probing [13]. This allows for the recovery of measurement errors of the robot's and its wrist's position sensors. Fig. 10 shows the composite tactile image of a 2-by-2 cluster of symbols on the top face of the object illustrated in Fig. 9.

The segmentation of the composite tactile image [15] allows recovery of 8-by-12 individual tactile images each of the four symbol in the 2-by-2 symbol cluster shown in Fig. 10.

A two-layer feedforward NN architecture with eight neurons in the hidden layer and four neurons in the output layer is then used to recognize the resulting 8-by-12 tactile images. The NN was trained using the gradient descent backpropagation algorithm with momentum [16], [17] and an adaptive learning rate

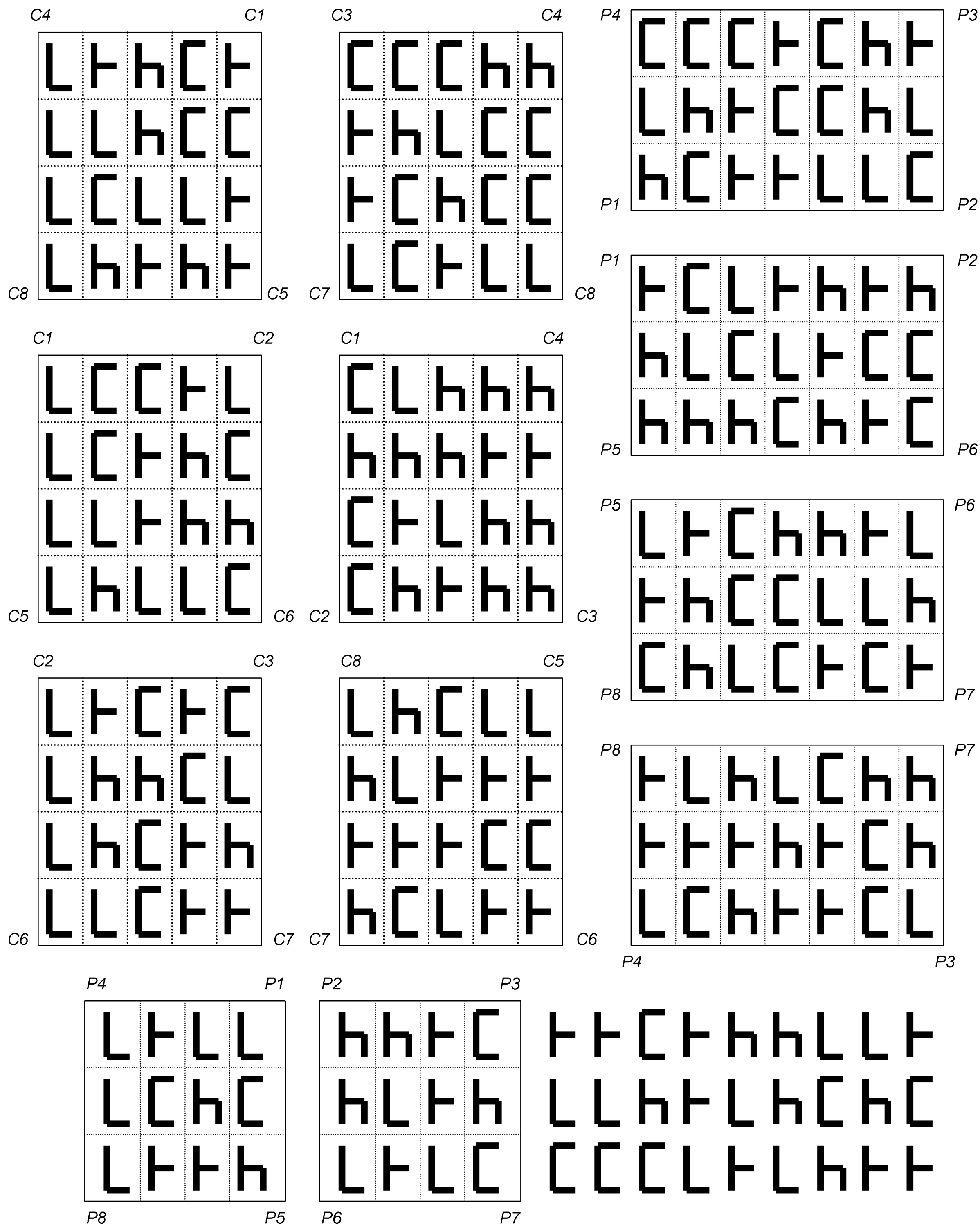

Fig. 8. Mapping the unfolded faces of the cube and the parallelepiped to the encoding PRA.

with a value of 0.95 for the momentum constant and a sum-squared-error goal of zero, for 5000 epochs. The network was trained with two real images of all characters, then with a real image corrupted by synthetic white random noise with a mean value of zero and standard deviations of 0.1, 0.15, and 0.2, respectively and then finally trained one more time with two other real images for each of the four characters.

Laboratory tests conducted over 500 real images of each of the four characters have resulted in a recognition rate of better than 99.6%.

To evaluate the generalization capability, the network was tested for different levels of white random noise with a mean value of zero and a standard deviation from 0 to 0.5 in steps of 0.05. Results over a set of 1100 synthetic test images for each

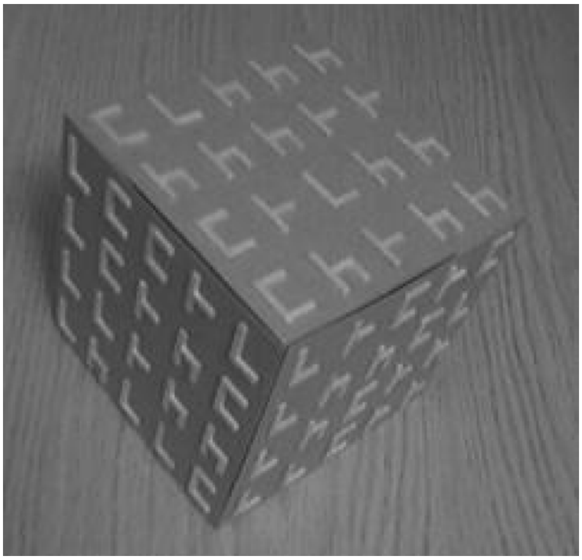

Fig. 9. The PRA encoded cube.

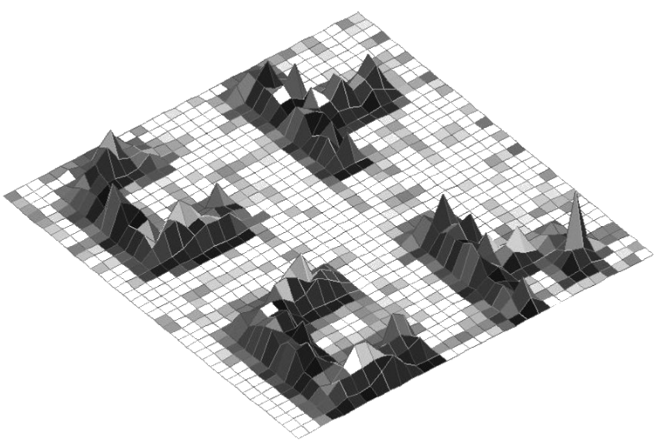

Fig. 10. Composite tactile image obtained by probing a 2-by-2 cluster of symbols embossed on the top face of the PRA encoded object shown in Fig. 9.

character have shown that the error rate for the recognition of any of the four embossing symbols was better than 0.6%. This relatively good error rate is due to the inclusion in the training process of the images corrupted by synthetic noise. When these noisy images were not used in training, the evaluation of the NN performance over the same set of 1100 synthetic test images has resulted in a maximum error rate of 2.1%.

The NN recognition of the tactile symbols recovered in Fig. 10 yields a 2-by-2 PRA window having the GF(4) values A^2 and A in the top row and A^2 and 1 in the second row. These window contents are unequivocally associated with the row–column coordinates $(i = 6, j = 5)$ of the upper left corner of this window within PRA. By searching the database that stores the object geometry/PRA mapping, illustrated in Fig. 7, we find that the recovered window belongs to the {C1, C2, C3, C4} face of the cube in the C2 corner as shown in Fig. 11.

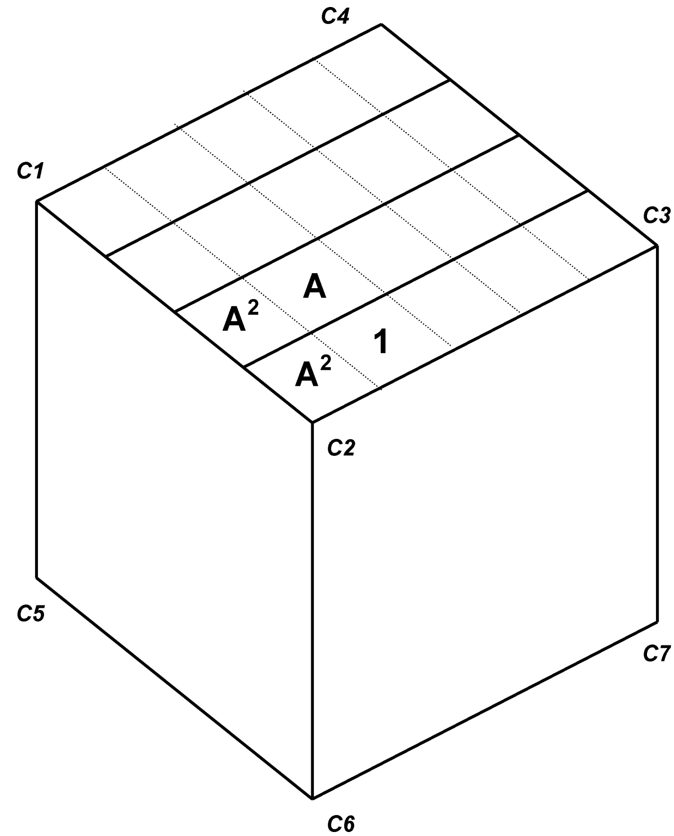

Fig. 11. The four symbols in the composite tactile image are recognized as representing the $\{A^2, A, A^2, 1\}$ GF(4) values. These window contents allow one to unequivocally identify the explored object face as being the {C1,C2,C3,C4} face of the cube, mapped to the encoding PRA as shown in Fig. 8.

V. Conclusions

The proposed model-based object recognition method was tested on two 3-D polyhedral objects: a cube and a parallelepiped.

While inherently restricted to a limited set of objects that have to be properly embossed with symbols arranged in a PRA pattern, the proposed method allows for a simple and robust blind object recognition using touch sensing only.

The use of a 15-by-17 PRA defined over GF(4), with $k1 = 2$ and $k2 = 2$, allows for a compact encoding that requires the recognition of only four symbols out of the 255 symbols of the whole PRA in order to unambiguously identify the object face and the exact position of the recovered symbols on this face. The compactness of the multivalued PRA encoding becomes even more evident for larger arrays. For instance, if $k1 = 2$ and $k2 = 3$, the encoding PRA defined over GF(4) will consist of 4095 symbols arranged in a 15-by-273 array, and will require the recognition of only six embossed symbols arranged in a 2-by-3 window pattern.

Simulation and experimental results have shown that the NN recognition of the tactile images has error rates better than 0.6% even in the case of images having up to a 50% noise ratio.

Despite its limitations, the proposed model-based robotic tactile object recognition technique has potential applications in environments where blind tactile sensing is the only sensing capability available.

ACKNOWLEDGMENT

The authors gratefully acknowledge the technical support provided by C. Pasca who helped with the development of the tactile probing system.

REFERENCES

[1] S. J. Lederman, R. L. Klatzky, and D. T. Pawluk, "Lessons from the study of biological touch for robotic haptic sensing," in *Advanced Tactile Sensing for Robotics*, H. R. Nicholls, Ed. Singapore: World Scientific, 1992.

[2] C. S. Tzafestas, "Whole-hand kinesthetic feedback and haptic perception in dextrous virtual manipulation," *IEEE Trans. Syst., Man, Cybern. A*, vol. 33, no. 1, pp. 100–113, 2003.

[3] P. Allen, "Integrating vision and touch for object recognition tasks," *Int. J. Robot. Res.*, vol. 7, no. 6, pp. 15–32, 1988.

[4] H. Petrie, V. Johnson, P. McNally, S. Morley, A.-M. O'Neill, and D. Majoe, "Inexpensive tactile interaction for blind computer users: two application domains," in *IEE Colloq. Developments in Tactile Displays*, 1997, Dig. 1997/012, pp. 2/1–2/3.

[5] J. Halousek, "Embossed Braille advancements: automatic "Reading" by a new optical Braille recognition system "OBR" and objective dot and paper quality evaluation," in *Proc. 14th Annu. Int. Conf. Technology and Persons With Disabilities*, 1999.

[6] J. Jurczyk and K. A. Loparo, "Mathematical transforms and correlation techniques for object recognition using tactile data," *IEEE Trans. Robot. Automat.*, vol. 5, no. 3, pp. 359–362, 1989.

[7] F. Germagnoli and G. Magenes, "A neural network-based system for tactile exploratory tasks," in *Proc. 1996 Int. Workshop Neural Networks for Identification, Control, Robotics, and Signal/Image Processing (NICROSP '96)*, Venice, Italy, 1996, pp. 458–466.

[8] F. J. MacWilliams and N. J. A. Sloane, "Pseudorandom sequences and arrays," *Proc. IEEE*, vol. 64, no. 12, pp. 1715–1729, 1976.

[9] R. Spann, "A two-dimensional correlation property of pseudorandom maximal-length sequences," *Proc. IEEE*, vol. 53, pp. 21–37, 1963.

[10] N. Trif, "Model-based visual recognition of 3-D Objects using pseudorandom grid encoding," M.A.Sc. thesis, University of Ottawa, Ottawa, ON, Canada, 1993.

[11] E. Petriu, W. S. McMath, S. K. Yeung, N. Trif, and T. Bieseman, "Two-dimensional position recovery for a free-ranging automated guided vehicle," *IEEE Trans. Instrum. Meas.*, vol. 42, no. 3, pp. 701–706, 1993.

[12] D. H. Ballard and C. M. Brown, *Computer Vision*. Englewood Cliffs, NJ: Prentice-Hall, 1982, ch. 9.

[13] E. M. Petriu, W. S. McMath, S. K. Yeung, and N. Trif, "Active tactile perception of object surface geometric profiles," *IEEE Trans. Instrum. Meas.*, vol. 41, no. 1, pp. 87–92, 1992.

[14] S. K. Yeung, E. M. Petriu, W. S. McMath, and D. C. Petriu, "High sampling resolution tactile sensor for object recognition," *IEEE Trans. Instrum. Meas.*, vol. 43, no. 2, pp. 277–282, 1994.

[15] R. Jain, R. Kasturi, and B. G. Schunck, *Machine Vision*. New York: McGraw-Hill, 1995, ch. 3.

[16] H. B. Demuth and M. Beale, *Neural Network Toolbox User's Guide*. Natick, MA: The MathWorks Inc., 1994.

[17] C. M. Bishop, *Neural Networks for Pattern Recognition*. Oxford, U.K.: Oxford Univ. Press, 1995, ch. 7.

Emil M. Petriu (M'86–SM'88–F'01) is a Professor in the School of Information Technology and Engineering, University of Ottawa, Ottawa, ON, Canada, where he has been since 1985. His research interests include test and measurement systems, interactive virtual environments, intelligent sensors, robot sensing and perception, neural networks, and fuzzy control. He has published more than 180 technical papers, authored two books, edited other two books, and received two patents.

Dr. Petriu is a Fellow of the Canadian Academy of Engineering and of the Engineering Institute of Canada. He is currently a member of the AdCom, Chair of TC-15 Virtual Systems, and Cochair of TC-28 Instrumentation and Measurement for Robotics and Automation of the IEEE Instrumentation and Measurement Society. He is an Associate Editor of the IEEE TRANSACTIONS ON INSTRUMENTATION AND MEASUREMENT and member of the editorial board of the IEEE I&M MAGAZINE.

Stephen K. S. Yeung, photograph and biography not available at the time of publication.

Sunil R. Das (M'70–SM'90–F'94–LF'03) received the B.Sc. (honors) degree in physics and the M.Sc.(Tech.) and Ph.D. degrees in radiophysics and electronics from the University of Calcutta, Calcutta, West Bengal, India.

He is a Professor of electrical and computer and computer engineering at the School of Information Technology and Engineering, University of Ottawa, Ottawa, ON, Canada. He has published extensibly in the areas of switching and automata theory, digital logic design, threshold logic, fault-tolerant computing, microprogramming and microarchitecture, microcode optimization, applied theory of graphs, and combinatorics. He edited (with P. K. Srimani) *Distributed Mutual Exclusion Algorithms* (Los Alamitos, CA: IEEE Computer Society Press, 1992) in its Technology Series. He is the author (with C. L. Sheng) of *Digital Logic Design* (Norwood, NJ: Ablex). He is a Member of the Editorial Board and a Regional Editor for Canada of *VLSI Design: An International Journal of Custom-Chip Design, Simulation and Testing*. He was Guest Editor of the *International Journal of Computer Aided VLSI Design* (September 1991), as well as *VLSI Design: An International Journal of Custom-Chip Design, Simulation and Testing* (March 1993, September 1996, and December 2001) Special Issues on VLSI Testing. He is an Associate Editor of the *International Journal of Parallel and Distributed Systems and Networks.*

Dr. Das is a Fellow of the Society for Design and Process Science and of the Canadian Academy of Engineering. He is a member of the IEEE Computer Society, IEEE Systems, Man, and Cybernetics Society, IEEE Circuits and Systems Society, and IEEE Instrumentation and Measurements Society. He is a member of the Association for Computing Machinery. He is the 1996 recipient of the IEEE Computer Society's Technical Achievement Award and the 1997 recipient of the IEEE Computer Society's Meritorious Service Award. He became a Golden Core Member of the IEEE Computer Society in 1998. He was a member of the IEEE Computer Society's Fellow Evaluation Committee in 2001. He is the recipient of the Rudolph Christian Karl Diesel Best Paper Award from the Society for Design and Process Science. He is the corecipient of the IEEE's Donald G. Fink Prize Paper Award for 2003. He was elected one of the delegates of "Good People, Good Deeds" of the R.O.C. in 1981 in recognition of his outstanding contributions in the field of research and education. He is listed in *Marquis Who's Who in the Computer Graphics Industry,* 1984. He was Managing Editor of the IEEE VLSI TECHNICAL BULLETIN and was an Executive Committee Member of the IEEE Computer Society Technical Committee on VLSI. He is currently an Associate Editor of the IEEE TRANSACTIONS ON SYSTEMS, MAN, AND CYBERNETICS, of the IEEE TRANSACTIONS ON INSTRUMENTATION AND MEASUREMENT. He is a former Administrative Committee (ADCOM) member of the IEEE Systems, Man, and Cybernetics Society, a former Associate Editor of the IEEE TRANSACTIONS ON VLSI SYSTEMS, a former Associate Editor of the *SIGDA Newsletter,* and a former Associate Editor of the *International Journal of Computer Aided VLSI Design*. He was Cochair of the IEEE Computer Society Students Activities Committee from Region 7 (Canada). He was Associate Guest Editor of the IEEE JOURNAL OF SOLID-STATE CIRCUITS Special Issues on Microelectronic Systems. He is currently Guest Editor (with R. Rajsuman) of a Special Issue of the IEEE TRANSACTIONS ON INSTRUMENTATION AND MEASUREMENT in the area of VLSI testing (Innovations in VLSI Test Equipments).

Ana-Maria Cretu (S'04) received the master's degree from the School of Information Technology and Engineering, University of Ottawa, Ottawa, ON, Canada, where she is currently pursuing the Ph.D. degree.

Her research interests include neural networks, robotic tactile sensing, 3-D object modeling, and multisensor data fusion.

Hans J. W. Spoelder, photograph and biography not available at the time of publication.